Propagation properties for a message in a Brownian sensor network

Niklas Gunnarsson
Dept. of Mathematics
Uppsala University
Box 480 SE 751 06 Uppsala
Sweden
Email: niklas@math.uu.se

Ingemar Kaj
Dept. of Mathematics
Uppsala University
Box 480 SE 751 06 Uppsala
Sweden
Email: ikaj@math.uu.se

Petteri Mannersalo
VTT Technical Research
Centre of Finland
P.O.Box 1000, 02044 VTT
Finland
Email: petteri.mannersalo@vtt.fi

***Abstract*— A wireless multi-hop sensor network, in which node positions are fixed, may fail to transmit a message over longer distances. This could occur, for example, due to low node density or small node transmission range. In mobile systems where nodes are allowed to move, it is natural to expect a better reachability, with the condition that messages are not time-critical and longer propagation delays are permitted. In order to understand the relation of mobility to node density and node transmission range, we study a simple network model where active sensors move according to independent Brownian motions. In the one-dimensional case, the propagation of a message can be viewed as a Brownian growth process among Poisson points on the real line. We investigate the distributional properties of the mobile nodes and show that the system grows linearly at a remarkably uniform rate. For the spatial model where planar Brownian motions transport and transfer the message to those nodes which eventually come within transmission range of active messenger nodes, we provide a discussion and some insight based primarily on simulations.**

I. INTRODUCTION

A number of studies have been devoted to the performance of wireless multi-hop networks such as ad hoc, hybrid, and sensor networks (see e.g. [5], [1], [4], [3]). A typical modeling assumption is that the nodes are distributed according to a spatial Poisson point process and once the locations are decided they are fix. If each Poisson point is the center of a closed ball of fix or independent and identically distributed radius, we have a Poisson Boolean model. These in turn lead to network models by interpreting the radius of the balls properly in terms of node transmission range.

A dynamic Boolean model is studied in [10]. Dynamic sensor networks are considered more recently in [2], where sensors switch their radio transmitters on and of randomly, and in [7], where the sensors move according to Brownian motions in segments with reflecting boundaries.

The often cited catch phrase *Mobility Increases the Capacity of Wireless Networks* which originates from [8] suggests that if some extra delay is permitted then mobility of the network nodes may improve network capacity and performance. However, there are few mathematical results available which make precise what that really means. In this study we present some preliminary results obtained in the case of one-dimensional models under Brownian mobility patterns. Possibly, knowing the rigorous behavior in such restricted cases may help us understand the role of mobility in general networks. As an additional part of this contribution, we discuss some topics for more general network models based on simulations.

The basic set-up in this paper is a Poisson Boolean model in which sensor nodes are placed according to a spatial Poisson process and have a fixed range of transmission. We consider idealistic communication links where a message is instantly transmitted when two nodes are within transmission range of each other. This approximates the situation, where the package to be transmitted is very small and the delays caused by processing and sending (in MAC and physical layer) are small compared to other delay sources, like the average time to get connected. Thus, two nodes communicate if their locations are at most the radius of transmission apart, i.e., in a Poisson Boolean model two balls with radius half the transmission range overlap. A node which receives a message immediately starts to broadcast this message, and continue to do so during the evolution of the system. To model the mobility, the nodes which carry the message move along paths of independent Brownian motions. The remaining nodes are assumed immobile, partly to make the analysis more transparent. This is in contrast to [10] where all nodes move simultaneously.

To understand how a message propagates through the network, consider a collection of sensors placed initially at the points of a Poisson point process in space. Suppose that a single sensor receives a message, that is, the sensor observes an event or obtains information which needs to be forwarded. This activates the sensor which starts performing a Brownian motion. As soon as one of the neighboring sensors is within transmission range of the messenger, the message is passed on. The messenger continues its movement, the newly activated node becomes mobile and performs a Brownian path independent of that of the messenger. The mechanism repeats itself as the message keeps reaching nodes at farther distances and the sensors which carry the message are allowed to move as independent Brownian motions. Hence, we expect the number of active messenger nodes, the Brownian sensors, to increase and the message to spread to further nodes successively in the form of a growing tree of branching Brownian motions.

Since the sensor locations of the original Poisson point process may be within transmission range of each other, we note also that several nodes may become activated at the same time epoch hence generating a tree-structure with a random offspring distribution.

We will report preliminary analytical results restricted to the case of zero transmission range in one dimension. In such non-radio networks transmissions occur at time points where a Brownian sensor hits a sensor not yet activated. In this case all message transmission times correspond to binary branching points. Our analysis refers to the asymptotic growth rate at which the system is able to transfer messages between nodes. The results rely on an application of Liggett's ergodic theorem for subadditive sequences together with analytic results for the distribution of the transmission times and the locations of the mobile nodes at transmission. In particular, we compute the expected time required for a message to reach a finite number of nodes. It turns out that the expected time between any two successive message transmission events is a constant independent of the number of Brownian sensors. Thus, the system grows at a highly regular linear rate.

Other topics are studied via simulations. These include the variance structure of the growth times, the change of behavior for the corresponding radio network, and the speed of propagation in the two-dimensional case. The remainder of the paper is structured in three sections. First we present in some detail model, exact results and asymptotic results for the one-dimensional model with zero transmission range. Section three contains a non-rigorous discussion devoted to radio networks. In the final section we discuss a model where active sensors move as independent Brownian motions with drift.

II. Non radio network

This is a version of the model where the functionality of the nodes is restricted to their mobility. This means that active nodes must reach the exact location of a neighboring, dormant node before being able to carry out their task of transmitting the message further through the system. In particular, since Brownian sensors in two or more dimensions never visit a single point, this means that non-radio networks only make sense in one dimension. In contrast, with positive probability a Brownian sensor reaches any open ball around a dormant sensor. This corresponds to radio networks where two sensors exchange a message at the first time the distance between them is at most the radius of transmission.

A. Model

Consider sensors distributed on the real line according to a Poisson process with constant intensity $\lambda > 0$. Hence, the distances between two adjacent sensors are independent and exponentially distributed with parameter λ (expected value $1/\lambda$). Designate one sensor to carry a message and denote by V_1 and V_2 the distances to its nearest neighbors, see Figure 1. At time $t = 0$ the messenger sensor starts performing a driftless Brownian motion such that the variance of its displacement from the initial position at time t is $\sigma^2 t$. Thus,

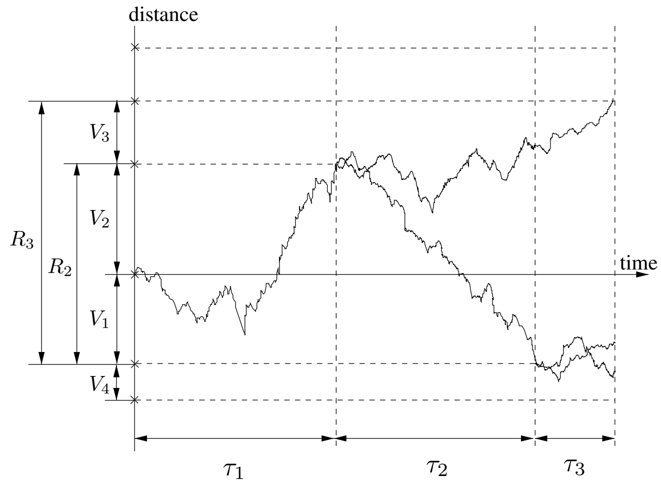

Fig. 1. Realization of the process until the third branching.

$\sigma^2 > 0$ is a mobility parameter. The dynamics of the non-radio version of the model is as follows. When the mobile sensor hits for the first time one of the dormant nearest neighbors, it forwards the message thereby activating the neighbor node, which immediately starts to move as an independent copy of the initial Brownian sensor. Denote by τ_1 the random time of activation of the second sensor. Assuming that the sensor up (down) from the moving sensor was reached first, let V_3 be the distance at time τ_1 between this sensor and its closest neighbor up (down). The next transmission and creation of a third Brownian sensor occurs when one of the Brownian sensors reaches for the first time the next dormant sensor, either up or down. Let τ_2 be the duration of the time interval during which there are exactly two Brownian sensors. This construction can be continued such that for each $k \geq 1$, τ_k is the length of time during which there are k Brownian sensors in the system which move over an interval of length R_{k+1}, where $R_k = V_1 + \cdots + V_k$ has the gamma distribution with parameters k and λ, $R_k \in \Gamma(k, \lambda)$, compare Figure 1. Note that mobile sensors are supposed to pass each other freely. What triggers branch point k is that anyone of the k Brownian sensors for the first time exits the corresponding interval of length R_{k+1}.

Our first step towards analyzing the sequence $\{\tau_k\}$ is to rescale the Brownian motions. Rather than an exit problem for k Brownian motions on an interval of length R_{k+1} this yields an exit problem on the interval $(0,1)$. We begin with the case $k = 1$. We may view the initial messenger node as a Brownian motion which starts at the distance V_1 from the origin and which is stopped at the first time of exit from the interval $(0, R_2)$. It is well-known that the relative starting point $X_1 = V_1/(V_1+V_2)$ is uniformly distributed on $(0,1)$ and that X_1 and R_2 are independent. Let $B(t)$ denote a standard Brownian motion, that is, a driftless Brownian motion which starts in zero at time $t = 0$ and has mobility parameter $\sigma^2 = 1$. Then

$$\tau_1 \quad = \quad \inf\{t > 0 : V_1 + \sigma B(t) \notin (0, R_2)\}$$

$$\stackrel{d}{=} \quad \inf\{t > 0 : X_1 + B(\sigma^2 t)/R_2 \notin (0,1)\}$$
$$\stackrel{d}{=} \quad \frac{1}{\sigma^2} R_2^2 \inf\{t > 0 : X_1 + \widetilde{B}(t) \notin (0,1)\},$$

where $\widetilde{B}(t) = B(R_2^2 t)/R_2$ is again a standard Brownian motion, which is independent of R_2 by Brownian scaling. By similar arguments we obtain for $k \geq 2$ the representation

$$\tau_k \stackrel{d}{=} \frac{1}{\sigma^2} R_{k+1}^2 \min_{1 \leq i \leq k} T_{k,i},$$

where

$$T_{k,i} = \inf\{t > 0 : X_{k,i} + B_{k,i}(t) \notin (0,1)\}, \quad 1 \leq i \leq k.$$

Here, $(X_{k,1}, \ldots, X_{k,k})$ are the ordered relative positions in $(0,1)$ obtained as initial positions when the k Brownian sensors at time $\tau_1 + \cdots + \tau_{k-1}$ are scaled from the interval of length R_{k+1}, and $\{B_{k,i}, 1 \leq i \leq k\}$ are independent standard Brownian motions which are also independent of $(X_{k,1}, \ldots, X_{k,k})$.

The time until n Brownian sensors have been activated is given by $S_n = \sum_{k=1}^n \tau_k$. Figure 2 shows a realization of the growth process until time S_{50}.

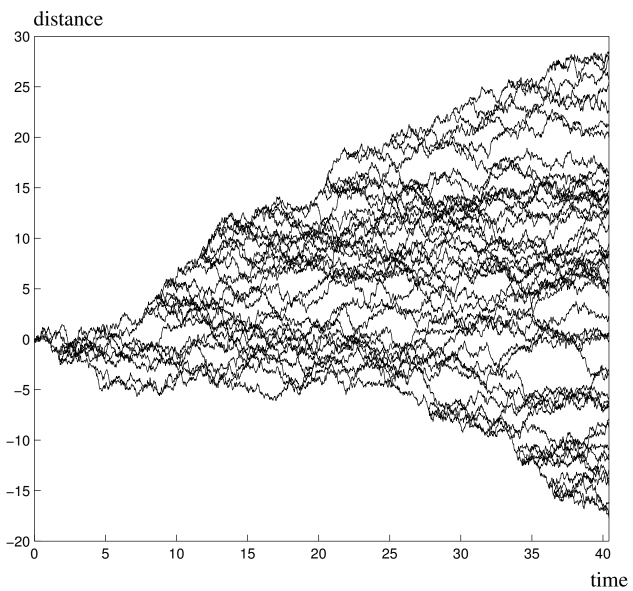

Fig. 2. Simulation of Brownian sensor process until time S_{50}. Initial message at origin, $\lambda = 1$, $\sigma = 1$.

B. Exact results

We are now prepared to state our results for the distribution of the location of the Brownian sensors at the message transmission times, and for the expected time duration between such transmissions.

Theorem 1: For each $k \geq 1$, the locations of sensors at the time when the kth sensor is activated is distributed on an interval of length $R_{k+1} \in \Gamma(k+1, \lambda)$, such that the relative positions of the sensors are independent of R_{k+1} and given for $k = 1$ by the uniform distribution $X_{1,1} \in U(0,1)$, and for $k \geq 2$ in increasing order by the vector

$$(X_{k,1}, \ldots, X_{k,k}) \stackrel{d}{=} \begin{cases} (U_{(1)}, U_{(1)}, \ldots, U_{(k-1)}), & \text{pr. } 1/2 \\ (U_{(2)}, \ldots, U_{(k)}, U_{(k)}), & \text{pr. } 1/2, \end{cases}$$

where $(U_{(1)}, \ldots, U_{(k)})$ is an ordered sample of k uniformly distributed points on the unit interval. Moreover, the expected time during which there are k active sensors is given by

$$E\tau_k = \frac{1}{\sigma^2 \lambda^2}, \quad k \geq 1.$$

Comments on the proof. For $k = 1$ we have $\tau_1 = R_2^2 T/\sigma^2$, where $R_2 \in \Gamma(2, \lambda)$ is independent of $T = \inf\{t > 0 : X + B(t) \notin (0,1)\}$, which is a stopping time with respect to the filtration generated by $\{B(t)\}$ and $X \in U(0,1)$. By optional stopping,

$$\begin{aligned} ET &= E(X + B(T))^2 - EX^2 \\ &= E(0^2 \cdot (1 - X) + 1^2 \cdot X) - EX^2 = 1/6. \end{aligned}$$

Since $ER_2^2 = 6/\lambda^2$ we obtain $E\tau_1 = 1/(\sigma\lambda)^2$.

At time τ_1 the distance between the two possible candidates for being the next, third, Brownian sensor extends from length R_2 to length R_3. The two already activated Brownian sensors are at this time both located in the same point, the relative positions being with equal probabilities either $X_{2,1} = V_3/R_3$ or $X_{2,2} = (V_1 + V_2)/R_3$ (this is the option realized in Figure 1). The variables $X_{2,1}$ and $X_{2,2}$ have the same beta distributions, $\beta(1,2)$ and $\beta(2,1)$, respectively, as the order variables $U_{(1)}$, $U_{(2)}$ generated by $k = 2$ independent uniform points in $(0,1)$. It can be shown that the resulting relative positions at the next branch point, where the 3rd sensor is activated, are with equal probabilities either of the form $(U_{(1)}, U_{(1)}, U_{(2)})$ or $(U_{(2)}, U_{(3)}, U_{(3)})$. The general statement is obtained by induction.

Given the successive distributions of all $(X_{k,1}, \ldots, X_{k,k})$, the expected value $E\tau_k$ can be obtained by an application of Ito's formula to the function $x \to |x|^2$ in R^k and optional stopping of the corresponding martingale.

C. Asymptotic results

We will show that S_n, the activation time of n sensors, satisfies a strong law of large numbers. Indeed, S_n/n converges to a constant almost surely as $n \to \infty$. However, we have been unable to verify that the limit equals the expected value $1/(\lambda\sigma)^2$.

Our analysis is based on a corresponding strong law of large numbers for the one-sided rate of growth in the system. Enumerate the sensors arbitrarily $\ldots, m-1, m, m+1, \ldots$ in order of their Poisson positions on the real line. Define for arbitrary integers $m \neq n$, $T_{m,m} = 0$ and

$T_{m,n} =$ the activation time of sensor n if initially a message is injected in sensor m.

We may think of these variables modeling the required time for a message to be carried from one node to a distant other node with the help of Brownian sensors relaying the message step by step.

Theorem 2: There exists a strictly positive constant $\eta \in [1/(\lambda\sigma)^2, \infty)$ such that

$$\lim_{n\to\infty} \frac{1}{n} T_{0,n} = \eta \quad a.s.$$
$$\lim_{n\to\infty} \frac{1}{n} S_n = \eta/2 \quad a.s.$$

We conjecture that $\eta = 2/(\lambda\sigma)^2$. Simulations indicate that the convergence is very slow.

Comments on the proof. The existence of a rate constant η, $0 \leq \eta < \infty$, is a consequence of Liggett's subadditive ergodic theorem, [9]. To recall the conditions for existence of such an η, we first note that the basic subadditivity property for the collection of random variables $\{T_{m,n}\}$,

$$T_{0,n} \leq T_{0,m} + T_{m,n} \quad 0 \leq m \leq n,$$

is intuitively clear from Figure 3. The bold trajectories do not

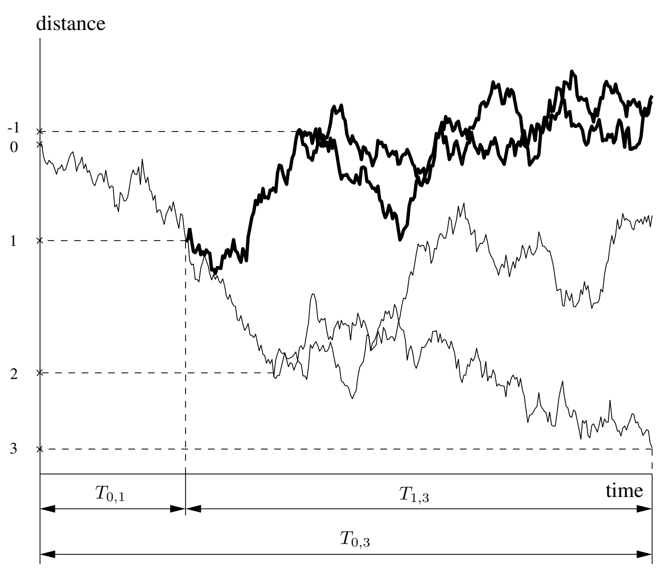

Fig. 3. Illustration of the inequality $T_{0,n} \leq T_{0,m} + T_{m,n}$ when $n = 3$,$m = 1$, the bold trajectories only affect $T_{0,3}$.

affect $T_{0,1}$ or $T_{1,3}$ but they have impact on $T_{0,3}$. In particular, $T_{0,3}$ will be less than $T_{0,1} + T_{1,3}$ if any of the bold trajectories reach sensor 3 before any of the thin trajectories do. By comparison with a simpler system and a coupling argument it can be shown that $ET_{0,n} < \infty$ for each n. Furthermore, the distribution of $\{T_{m,m+k}, k \geq 1\}$ does not depend on m, and for each $k \geq 1$, the sequence $\{T_{nk,(n+1)k}, n \geq 0\}$ is both stationary and ergodic. Based on these properties we obtain a rate constant defined by $\eta = \inf_{n\geq 1} ET_{0,n}/n$, for which holds $T_{0,n}/n \to \eta$, a.s.

Next, we may consider $\{T_{m,n}\}$ and $\{S_n\}$ defined on the same probability space, and observe the ordering $T_{0,n} \geq S_n$. Thus, by Theorem 1, $\eta \geq 1/(\lambda\sigma)^2$. Moreover,

$$\min(T_{0,n}, T_{0,-n}) \leq S_{2n} \leq \max(T_{0,n}, T_{0,-n}).$$

This yields,

$$\frac{1}{2}\min(\frac{T_{0,n}}{n}, \frac{T_{0,-n}}{n}) \leq \frac{S_{2n}}{2n} \leq \frac{1}{2}\max(\frac{T_{0,n}}{n}, \frac{T_{0,-n}}{n}),$$

where the expressions both on the left and the right side converges almost surely to $\eta/2$, and hence S_n/n converges almost surely to $\eta/2$. As an illustration, typical realizations of S_n and S_n/n are shown in Figure 4.

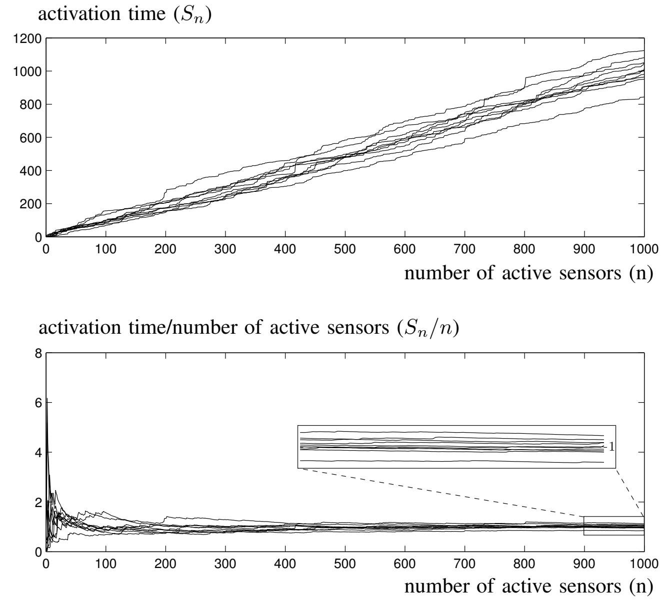

Fig. 4. Ten realization of S_n and S_n/n, $1 \leq n \leq 1000$, $\lambda = 1$, $\sigma = 1$.

To conclude our presentation of the non-radio network model, simulation results for the variance of S_n, $V(S_n)$, are shown in Figure 5. They provide evidence for the linear behavior $V(S_n) \approx Cn$, where $C \approx 8$.

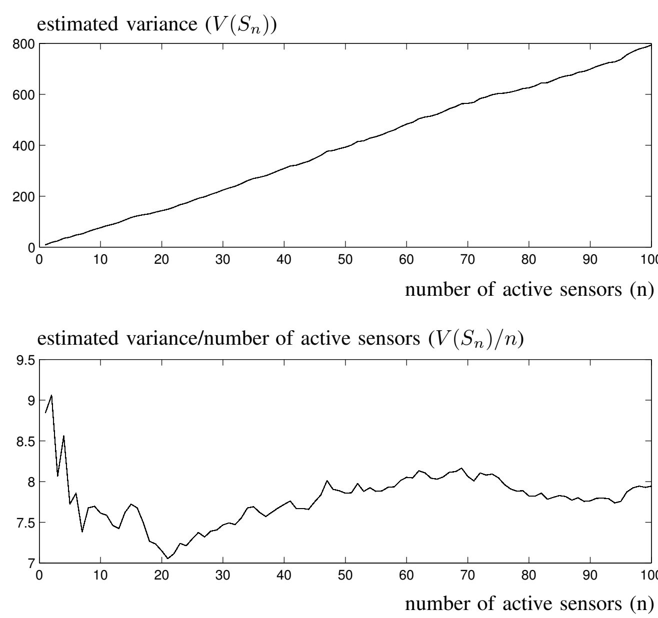

Fig. 5. Estimation of $V(S_n)$ and $V(S_n)/n$ in one-dimension, $\lambda = 1$, $\sigma = 1$.

III. Radio network

In this section we consider the situation when all nodes, active or not, have the ability to pick up the signal of, and react to, any other node within distance $r > 0$ of its own position. The parameter r is the transmission radius in the model. In this case, the critical intensity λ_c plays an important role: for $\lambda < \lambda_c$ the underlying Poisson Boolean model has only bounded connected components almost surely and for $\lambda > \lambda_c$ there is an unbounded connected component (i.e. infinite cluster) almost surely. These regimes are called subcritical and supercritical, respectively. In one dimension the Poisson Boolean model is always subcritical, whereas in higher dimensions both regimes exist.

A. Supercritical case

In the supercritical case, propagation of a message between two distant points usually consists of two steps. First the message must reach the underlying infinite cluster. If the target node belongs to the infinite cluster we are done. If not, one of the infinitely many Brownian sensors must find the target location. Only when the destination is very close to the origin, activation of the infinite cluster is not needed.

Any given point is either part of the infinite cluster or inside a hole of the infinite cluster. In two dimensions, the holes are bounded sets, almost surely. Since the exit time of Brownian motion from a bounded set has finite mean, the expected time to activate the infinite cluster in 2D is also finite. In dimensions three and higher, there are no bounded holes. Hence, Brownian sensors could spend much time away from the infinite cluster. Whether this implies that the time to activate the infinite cluster has infinite mean or not is currently unknown to us.

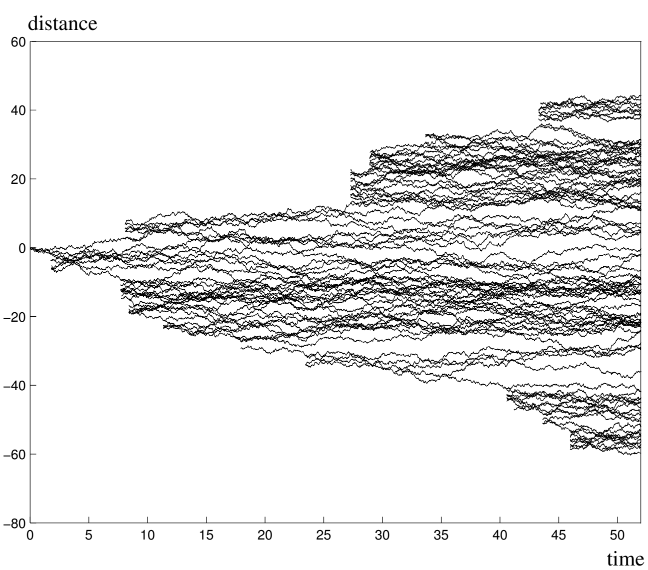

Fig. 6. Simulation of a 1-dimensional radio network until 100 active sensors, $\lambda = 1$, $\sigma = 1$, $r = 1.3$.

The second step consisting of movements of infinitely many Brownian sensors can possibly be analyzed using a Boolean model where the marks are the Wiener sausages $W_t \doteq \cup_{s \leq t} S(B_s, r)$, where $S(x, r)$ denotes a ball with center x and radius r.

B. Subcritical case

The radio transmission version of the one-dimensional model always performs better than the non-radio version, regarding message propagation properties. In principle, the speed of growth increases with the transmission radius, or put differently with the mean cluster size. This is visualized in Figure 6, where step wise branch points are visible corresponding to the simultaneous activation of a cluster of sensors within transmission range of each other.

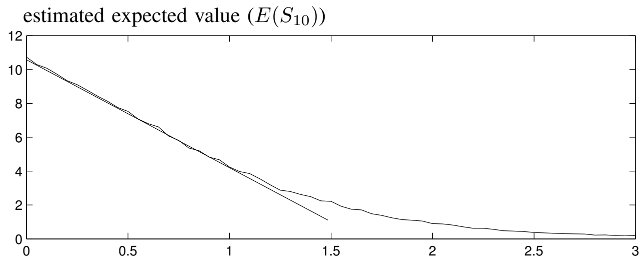

Fig. 7. Estimation of $E(S_{10})$ for different transmission radius in the one-dimensional model, $\lambda = 1$, $\sigma = 1$.

To comment on the qualitative aspects of the gain in propagation speed, our simulations suggest a nearly linear increase in the growth rate of the tree of Brownian sensors for small and medium transmission range. For larger values of the transmission range of the order of magnitude of the average distance between nodes the growth rate decreases. See Figure 7.

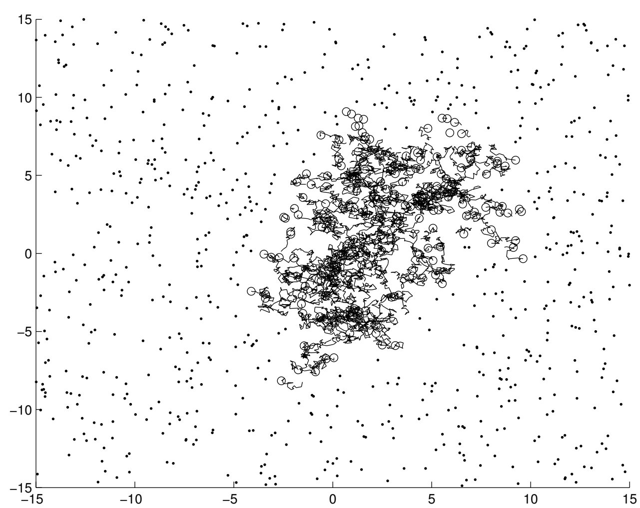

Fig. 8. Simulation of Brownian sensor process in two-dimensions $\lambda = 1$, $\sigma = 1$, $r = 0.6$.

Turning to the two-dimensional model, the planar Poisson radio model with subcritical intensity is illustrated in Figure 8. Here a message is initially placed in the origin and it propagates through the system relayed via Brownian sensors. The lines are the paths of the active sensors and the circles

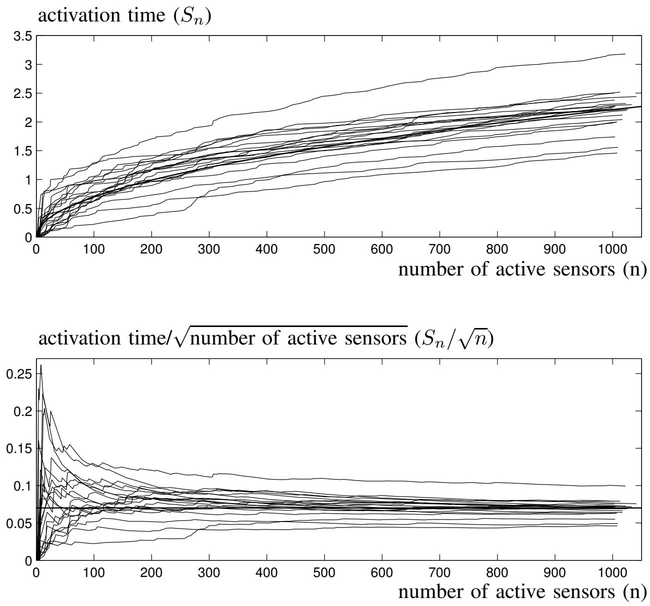

Fig. 9. S_n and $S_n/\sqrt{n}$ for 20 realizations of the Brownian sensor process in dimension 2, $\lambda = 1$, $\sigma = 1$, $r = 0.8$.

their positions at time S_{150} when a total of at least 150 sensors have been activated. The small dots represents the positions of dormant sensors.

Our simulations suggest in this case that

$$\mathrm{E}\left(S_n\right) \approx \frac{c_r \sqrt{n}}{(\sigma\lambda)^2}$$

where c_r is a constant that depends on the transmission radius. Figure 9 shows S_n and $S_n/\sqrt{n}$ for twenty independent realizations when $\lambda = 1$, $\sigma = 1$, the transmission radius $r = 0.8$, and the maximum n is slightly greater than 1000. The thick lines are $0.06\sqrt{n}$ and 0.06, respectively. As can be seen in Figure 9 the values of S_n for small n has big influence on S_n for large values on n, which is consistent with the slow convergence of $S_n/\sqrt{n}$ we observe.

IV. Further topics

A. Brownian motion with drift

The modeling assumption that active sensors move according to independent Brownian motions may seem unrealistic. Possibly, a more realistic model is to let the active sensors move as independent Brownian motions with drift. Consider a Brownian motion with randomly signed drift

$$\widetilde{B}_t = \sigma B_t + Z\mu t, \quad t \geq 0$$

where B_t is a standard Brownian motion, Z is a random sign of plus or minus one with equal probabilities, and μ is a constant drift term. For each sensor, the sign of the random drift is determined at the activation time of the sensor and kept fixed during the evolution of the system. For $\mu = 0$ we obtain the previous model where active sensors move as independent Brownian motions. Figure 10 shows a realization of a non-radio network in one dimension where active sensors

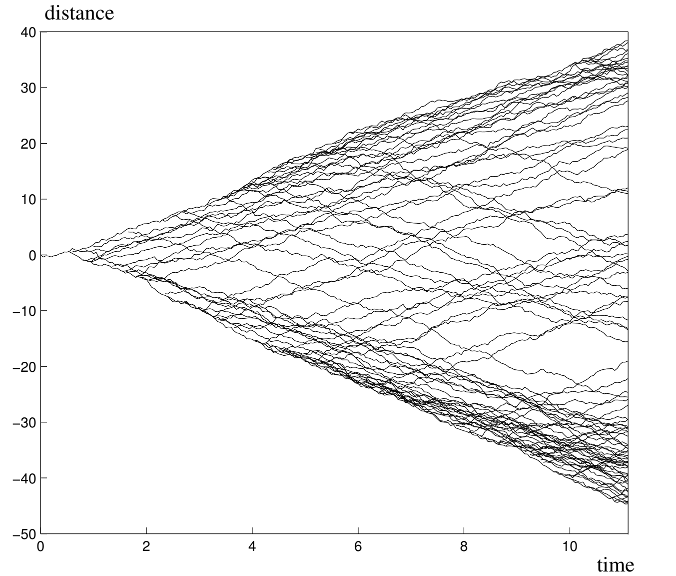

Fig. 10. Simulation of Brownian sensor process until time S_{200} $\lambda = 1$, $\sigma = 1$, $\mu = 3$.

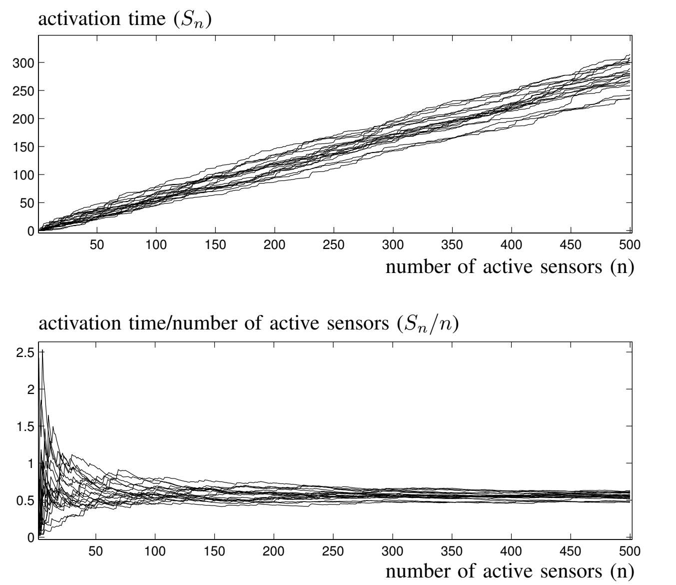

Fig. 11. Twenty realizations of S_n and S_n/n when $1 \leq n \leq 500$, $\lambda = 1$, $\sigma = 1$, $\mu = 0.4$.

move according to the above model of independent Brownian motions with randomly signed drift parameter $\mu = 3$. In this case the distribution of sensor locations seem to have a higher concentration near the ends of the interval of interest. This is in contrast to the case $\mu = 0$, where the Brownian sensors are distributed almost uniformly on the interval. With this in mind one can expect that the time to activate n sensors is smaller for a network with $\mu > 0$ than for a network with $\mu = 0$. Indeed, our simulations of S_n in Figure 11 verify that this is the case. For a large value of μ, such as $\mu = 3$ in Figure 10 where the ratio S_n/n seems to tend to a number between 0.12 and 0.13, the expected growth rate is substantially larger than in the case $\mu = 0$.

B. Higher dimensions

In three dimensions our simulations suggest that the time to activation of n sensors grows as a constant times $n^{1/3}$, see Figure 12. In one and two dimensions simulations show that the corresponding growth rate is a constant times n respective a constant times $n^{1/2}$. Thus we conjecture that S_n grows as $C(d)n^{1/d}$, where $C(d)$ is a constant and $d \geq 1$ is the dimension under consideration.

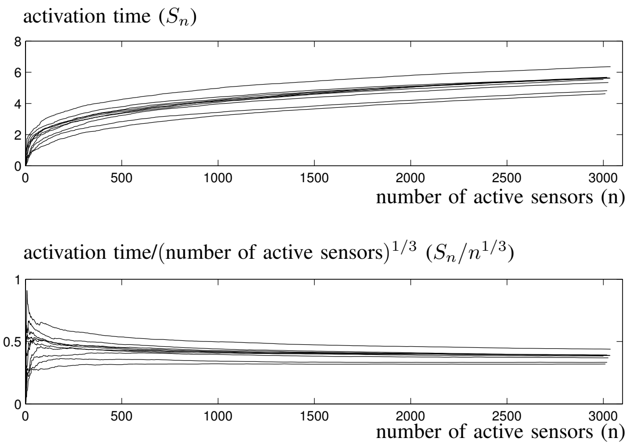

Fig. 12. Ten realizations of S_n and $S_n/n^{1/3}$ in three dimensions when $1 \leq n \leq 3000$, $\lambda = 1$, $\sigma = 1$, $r = 0.4$.

References

[1] L. Booth, J. Bruck, M. Franceschetti, and R. Meester, "Covering algorithm, continuum percolation and the geometry of wireless networks," *Ann. Appl. Probab.*, vol. 13, no. 2, pp. 722–741, 2003.

[2] O. Dousse, P. Mannersalo, and P. Thiran, "Latency of wireless sensor networks with uncoordinated power saving mechanisms," in *Proceedings of Mobihoc*, 2004, pp. 109–120.

[3] O. Dousse and P. Thiran, "Connectivity vs capacity in dense ad hoc networks," in *Proceedings of IEEE Infocom*, 2004.

[4] O. Dousse, F. Baccelli, and P. Thiran, "Impact of interferences on connectivity in ad hoc networks," in *Proceedings of IEEE Infocom*, 2003.

[5] O. Dousse, P. Thiran, and M. Hassler, "Connectivity in ad hoc and hybrid networks," in *Proceedings of IEEE Infocom*, New York, USA, 2002.

[6] M. Franceschetti, L. Booth, J. Bruck, M. Cook, and R. Meester, "Percolation in multi-hop wireless networks," *IEEE Trans. Inf. Theory*, 2003, submitted. A short version appeared at ISIT'03.

[7] R. Groenevelt, E. Altman, and P. Nain, "Relaying in mobile ad hoc networks: the Brownian motion mobility model," *Journal of Wireless Networks*, 2005, to appear.

[8] M. Grossglauser and D. Tse, "Mobility increases the capacity of ad hoc wireless networks," *IEEE/ACM Trans. Netw.*, vol. 10, no. 4, 2002.

[9] T. Liggett, "An improved subadditive ergodic theorem," *Ann. Probab.*, vol. 13, no. 4, pp. 1279–1285, 1985.

[10] J. van den Berg, R. Meester and D.G. White, "Dynamic Boolean models," *Stochastic Proc. Appl.* vol. 69, pp.247–257, 1997.